

## Investigation of polyelectrolyte desorption by single molecule force spectroscopy

This article has been downloaded from IOPscience. Please scroll down to see the full text article.

2004 J. Phys.: Condens. Matter 16 S2369

(<http://iopscience.iop.org/0953-8984/16/26/010>)

View [the table of contents for this issue](#), or go to the [journal homepage](#) for more

Download details:

IP Address: 129.252.86.83

The article was downloaded on 27/05/2010 at 15:40

Please note that [terms and conditions apply](#).

# Investigation of polyelectrolyte desorption by single molecule force spectroscopy

C Friedsam, M Seitz and H E Gaub

Lehrstuhl für Angewandte Physik and Center for NanoScience, Ludwig-Maximilians-Universität München, Germany

E-mail: Hermann.Gaub@physik.uni-muenchen.de

Received 7 May 2004

Published 18 June 2004

Online at [stacks.iop.org/JPhysCM/16/S2369](http://stacks.iop.org/JPhysCM/16/S2369)

doi:10.1088/0953-8984/16/26/010

## Abstract

Single molecule force spectroscopy has evolved into a powerful method for the investigation of intra- and intermolecular interactions at the level of individual molecules. Many examples, including the investigation of the dynamic properties of complex biological systems as well as the properties of covalent bonds or intermolecular transitions within individual polymers, are reported in the literature. The technique has recently been extended to the systematic investigation of desorption processes of individual polyelectrolyte molecules adsorbed on generic surfaces. The stable covalent attachment of polyelectrolyte molecules to the AFM-tip provides the possibility of performing long-term measurements with the same set of molecules and therefore allows the *in situ* observation of the impact of environmental changes on the adsorption behaviour of individual molecules. Different types of interactions, e.g. electrostatic or hydrophobic interactions, that determine the adsorption process could be identified and characterized. The experiments provided valuable details that help to understand the nature and the properties of non-covalent interactions, which is helpful with regard to biological systems as well as for technical applications. Apart from this, desorption experiments can be utilized to characterize the properties of surfaces or polymer coatings. Therefore they represent a versatile tool that can be further developed in terms of various aspects.

(Some figures in this article are in colour only in the electronic version)

## 1. Introduction

Polyelectrolytes are long chain molecules consisting of many identical subunits that acquire an electric charge upon dissolution in water. They play an important role in industrial as well as in biological processes [1–3]. In particular, their interaction with solid supports is the basis

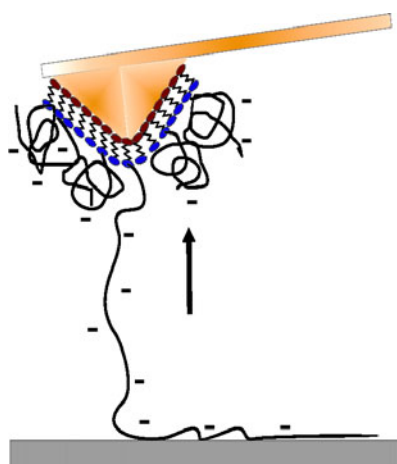


**Figure 1.** Setup of the experiment: the polyelectrolyte functionalized tip is opposing a generic surface. When the tip approaches the surface the polyelectrolyte is allowed to adsorb and when the tip is retracted the desorption process can be observed.

of numerous applications such as mineral separation [4], flocculation [5, 6] or retention [7]. In the field of biology the growth of biominerals, that is believed to be determined by specific interactions between biopolymers and the mineral surface, is just one example of a process that is mediated by polymer adsorption [8–11]. Due to its widespread occurrence and importance polyelectrolyte adsorption is the focus of interest for experimental research [12–22] as well as for theoretical considerations [23–29].

The adsorption process is often governed by electrostatic interactions of polyelectrolyte molecules with a charged surface, e.g. during the buildup of multilayered structures [30–33] or the adsorption of polyelectrolytes on charged membranes [34–37]. But there are also examples where non-Coulombic contributions are of critical importance, e.g. concerning the interaction of polyelectrolytes with hydrophobic surfactants [38, 39]. Therefore it is an important goal to distinguish between different types of interactions involved in polyelectrolyte adsorption in order to identify their impact and obtain a background that helps to understand the nature of specific adsorption processes. In the course of this report we will show how single molecule force spectroscopy can be utilized to isolate different contributions and elucidate their role in the investigated adsorption process.

## 2. Single molecule force spectroscopy

Over the past 15 years a variety of different experimental techniques have been developed that are capable of determining the interaction forces between individual molecules [40–43]. One of them is AFM-based single molecule force spectroscopy [44]. It allows the measurement of intra- and intermolecular forces [45–50] ranging from the pN regime, e.g. for receptor–ligand systems [51–53] to the nN regime that is reached when single covalent bonds are ruptured [54]. Recently polyelectrolyte desorption has been introduced as a subject of investigation in single molecule force spectroscopy [20–22]. Figure 1 shows one possible realization of such a desorption experiment: the polyelectrolyte molecules are grafted to an AFM-tip that is opposing a generic surface. When the tip approaches the surface the polyelectrolyte molecules are allowed to adsorb onto the surface; when it is retracted the desorption force that belongs to the desorption of one or a few individual molecules is measured.

Typically, in desorption, measurements plateaux are found in the force-extension curves. This is quite in contrast to most of the other systems investigated so far that show the stretching

curve of a polymer spacer, terminated by the rupture of one single specific bond. If ruptures are observed the measurements take place under non-equilibrium conditions and the rupture forces depend on the force loading rates [55–61]. The rupturing of the investigated bonds is an irreversible process. Non-equilibrium conditions can be observed if the time that is required in the experiment to exert a force that is strong enough to induce bond rupturing is comparable to the natural lifetime of the bond. Two main reasons may be considered to explain the observation of desorption plateaux. If the polymer spacer carries a series of binding sites the shape of the resulting force–extension curve depends strongly on the distance between two neighbouring binding sites. With a decreasing distance between the ruptured bonds it becomes more difficult to resolve the single ruptures and finally their overlay results in a plateau-like shape. In this case the measurements still take place in non-equilibrium. The height of the plateau is loading-rate dependent and therefore the observed histogram of the desorption forces is not Gaussian. A second reason for the occurrence of desorption plateaux is due to kinetic arguments. If the bonds involved in the adsorption process dissociate and re-associate on a much faster timescale than the experimental pulling process occurs, it is not possible to stretch the polymer spacer connecting two neighbouring bonds and therefore no rupture events are observed. Instead of this one ends up with a constant equilibrium desorption force that reflects the process of peeling off the polymer from the surface segment by segment. The measurement then takes place in thermal equilibrium; no loading rate dependence is observed and the investigated process is reversible. Therefore the histogram of the desorption forces is Gaussian. All experiments reported here corresponded to this case. The three described scenarios are illustrated in figure 2.

Figure 3 shows a typical force–extension curve of a desorption experiment and its analysis. Two different steps were recorded that represent the desorption of two individual molecules of different length. Each time one polymer strand is completely desorbed a step in the desorption force is recorded until the last polymer is fully detached. The plateau length directly reflects the length of an adsorbed polymer, whereas the height of a plateau corresponds to the desorption force that is required to desorb one or multiple polymers from the opposing surface. The heights of the plateaux are collected in a desorption force histogram that shows one or more narrow Gaussian distributions. The peaks of these distributions represent the mean desorption force that is required to desorb one or more polyelectrolyte molecules from the opposing surface. As the polyelectrolyte molecules generally show broad length distributions, that are hard to interpret, the desorption lengths are not collected in a histogram. Instead of this the lengths of all desorption plateaux observed in a desorption experiment are plotted against their curve number. In this type of depiction it is easier to correlate differences in the observed desorption lengths with changes in the environmental conditions.

### 3. AFM-tip functionalization for long-term measurements

The preparation and functionalization of long-term stable polymer coated AFM-tips generally is an important issue in force spectroscopy. In particular, in the context of desorption experiments it is a desirable goal to reach long-term stability because it provides the opportunity to measure a long series of desorption curves with the same set of molecules under various experimental conditions. Therefore deviations due to different sample preparations can be ruled out and the results can be directly compared. The most common method for AFM-tip functionalization is silanization, which was applied successfully in many cases [54, 62, 63]. But ageing and wearing of the silane layer were frequently found to limit the use of such tips in long-term measurements. A favourable alternative to silanization is the use of thiol chemistry on gold surfaces. Quite in contrast to the silanization process on silicon nitride [64–67], it is

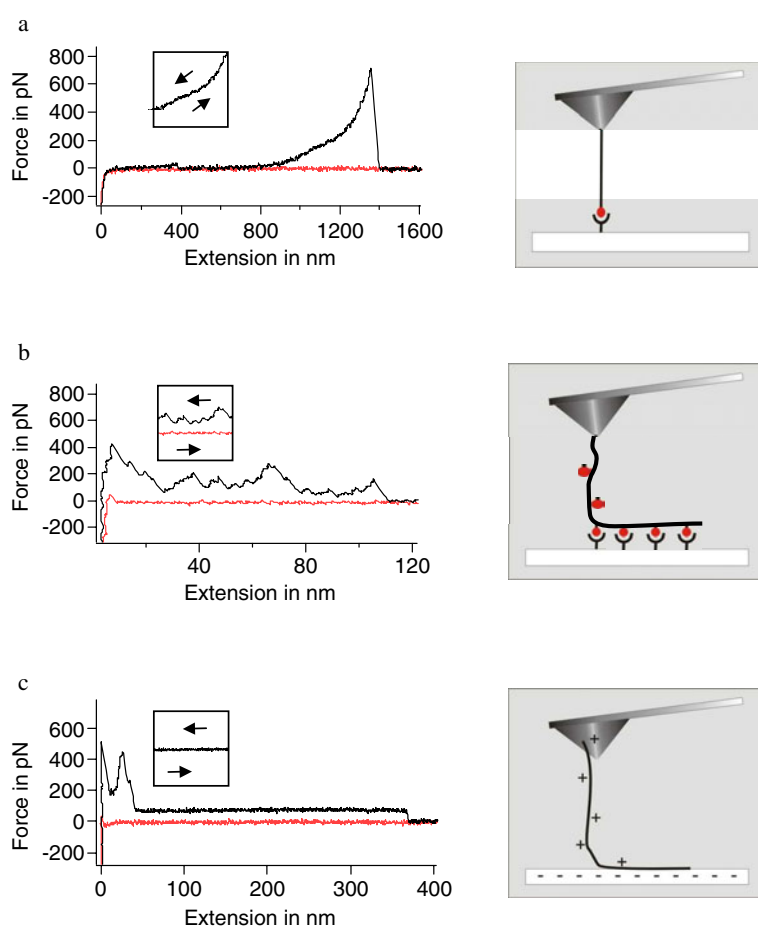


**Figure 2.** Different shapes of force-extension curves and their explanation. The inset shows examples for reversible and irreversible processes. (a) Rupturing of one specific bond coupled to a polymer-spacer in a non-equilibrium process. As its natural lifetime is sufficiently high the bond remains closed during the whole pulling process. Thus the stretching of the polymer spacer is observed until the bond is ruptured by the applied force. The rupturing of the bond is an irreversible process whereas the stretching of the polymer spacer is reversible: one can go back and forth on the force curves and re-measure the stretching of the polymer without hysteresis. (b) Rupturing of numerous bonds in series in a non-equilibrium process. If the distance between the different binding sites on the polymer spacer becomes smaller and smaller it becomes more and more difficult to resolve the single rupture events and the force-extension curve approaches a plateau-like shape. The rupturing of the bonds is an irreversible process. One has to approach the surface again at zero force in order to measure the rupturing of the bonds repeatedly. (c) Rupturing of numerous bonds in series in an equilibrium process. The individual bonds dissociate and re-associate on a much faster timescale than the experimental pulling process occurs and the stretching of the polymer spacer can no longer be observed. Instead of this one observes a desorption plateau whose height reflects the equilibrium desorption force required to peel the polymer off the surface segment by segment. The desorption of the polymer is a reversible process; it is possible to go back and forth on the desorption plateau.

rather straightforward to produce well-defined and densely packed monolayers of mercapto-terminated alkyl-chains on gold [68–70]. This fact was utilized to remarkably enhance the long-term stability of functionalized AFM-tips. The technique could be successfully applied

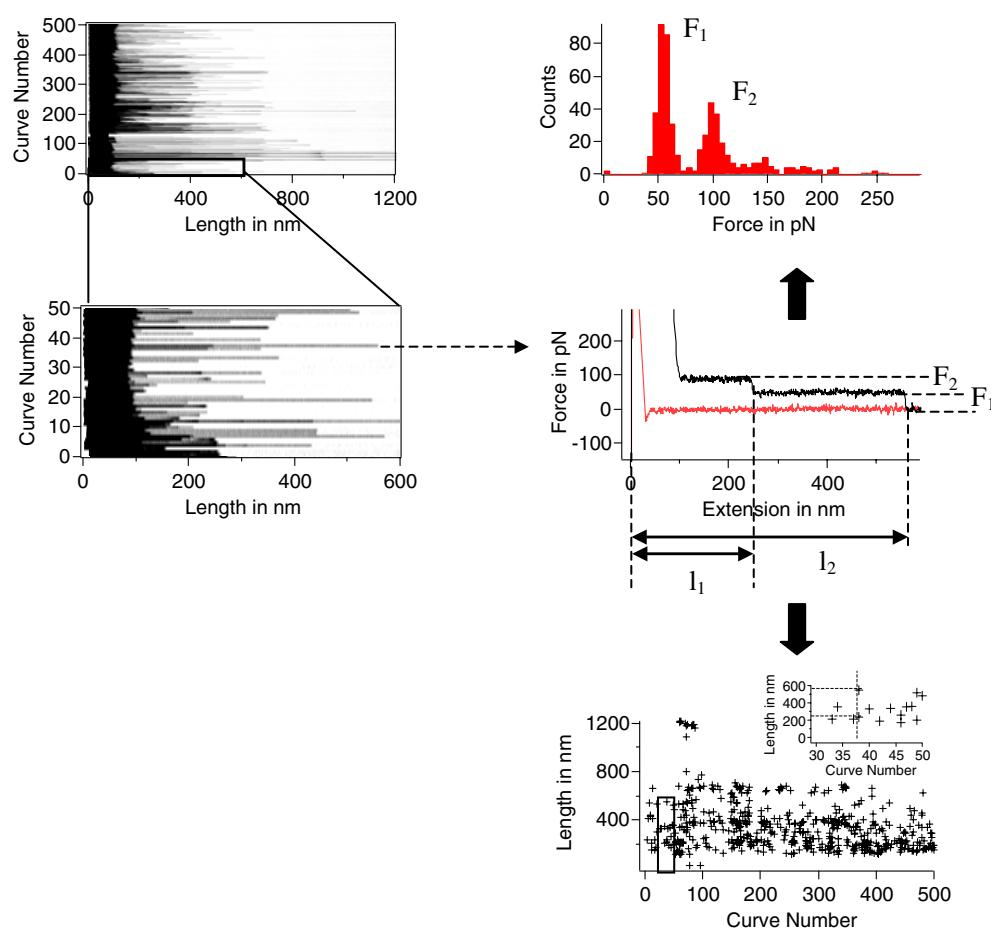


**Figure 3.** Analysis of the force-extension curves. A couple of desorption curves are measured under certain environmental conditions. They are shown as an image plot where the curve number is plotted against the length and the force is converted into a grey scale. The analysis is shown in an example of one force-extension curve which shows the desorption of two molecules of different lengths. The heights of the two plateaux reflect the force that is required to desorb two and one individual polyelectrolyte molecules from the surface, respectively. Multiples of such events are collected in a desorption force histogram that shows different peaks corresponding to the desorption process of one or more individual molecules. The mean desorption force that is required to desorb one individual polyelectrolyte molecule from the surface can be determined by a Gaussian-fit of the first peak in the histogram. The lengths of the plateaux correspond to the lengths of the desorbed polymers. They are plotted against their curve number in order to monitor changes of the desorption lengths in the course of time, which can be correlated with environmental changes.

to bind polymers with carboxyl groups as well as polymers with amines via peptide bonds to an AFM-tip [71]. The whole process is illustrated in figure 4 for the case of polyacrylic acid.

For several reasons, desorption experiments themselves provide a suitable method to characterize the capability of the polymer coating to withstand long-term measurements. As the desorption processes we investigated so far were found to be rate-independent and typically showed very narrow Gaussian force distributions, possible disturbances that would broaden these narrow distributions, e.g. from contaminations, can be easily identified. The adsorption-desorption process is mediated by a weak reversible binding process and the corresponding

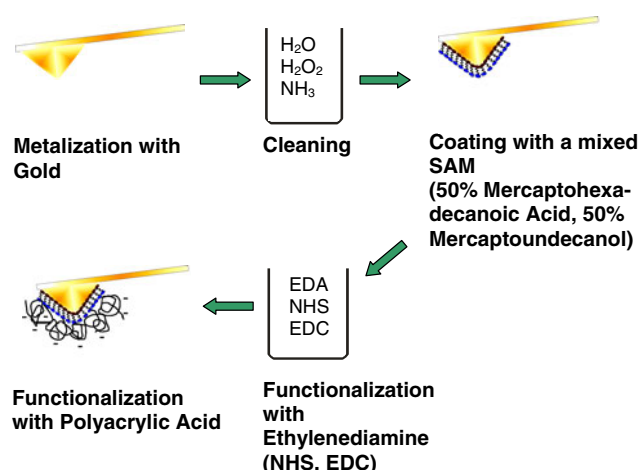


**Figure 4.** Preparation of the polyacrylic acid functionalized tips. First the cantilevers were coated by thermal evaporation with 10 nm of chrome–nickel (80:20) followed by 40 nm of gold. Then they were cleaned in a mixture ( $v/v/v = 5:1:1$ ) of deionized water, ammonia (30 vol%), hydrogen peroxide (25 vol%) at 70 °C for at least one hour (caution: the solution causes severe burns!). After this they were incubated in a solution of 1 mM 11-mercaptoundecan-1-ol 100 ml ethanol (puriss.) for 24 h. The carboxy functions of the resulting self-assembled thiol monolayer were then reacted with ethylenediamine and finally functionalized with polyacrylic acid.

desorption forces are one order of magnitude weaker than the covalent intramolecular bonds of the polymer. The polymer structure is thus not affected by the desorption process. As a consequence, the general stability of the polymer coated tips with respect to environmental influences and ageing could be monitored in such experiments.

Concerning the long-term stability of the AFM-tips, we focused on three possible reasons for degradation and the related experimental consequences:

- (1) if one or several probe molecules detached from the tip during the measurements, the number of adsorption events would decrease;
- (2) tip contamination would result in broad and undefined distributions of the desorption forces;
- (3) if the molecules formed additional unspecific bonds with the AFM-tip that are stronger than the bonds with the underlying substrate, their desorption length would decrease.

The desorption length, the number of desorption events and the shape of the desorption force histograms can therefore be used as criteria to exclude these degradation effects of the polymer coated tips.

A typical example of such long-term measurement is shown in figure 5. Figure 5(a) shows the development of the desorption lengths for a polyacrylic acid coated tip on various substrates (COOH, OH, CH<sub>3</sub>-SAM, gold, glass, calcite, mica) with CaSO<sub>4</sub> in solution. About 40 000 force spectra were recorded. For the measurement as a whole, no systematic decrease in desorption length could be recorded and therefore one can conclude that the polymer coating remains stable and no significant unspecific binding to the tip occurred during the measurement. In figure 5(b) the development of the desorption forces corresponding to the measurements shown in figure 5(a) is plotted. Three desorption force histograms are extracted, one at the beginning, one in the middle and one at the end of the measurements. In each case 500 force spectra contribute to the desorption force histogram. Every histogram shows a narrow Gaussian peak that corresponds to the desorption of a single polymer chain from

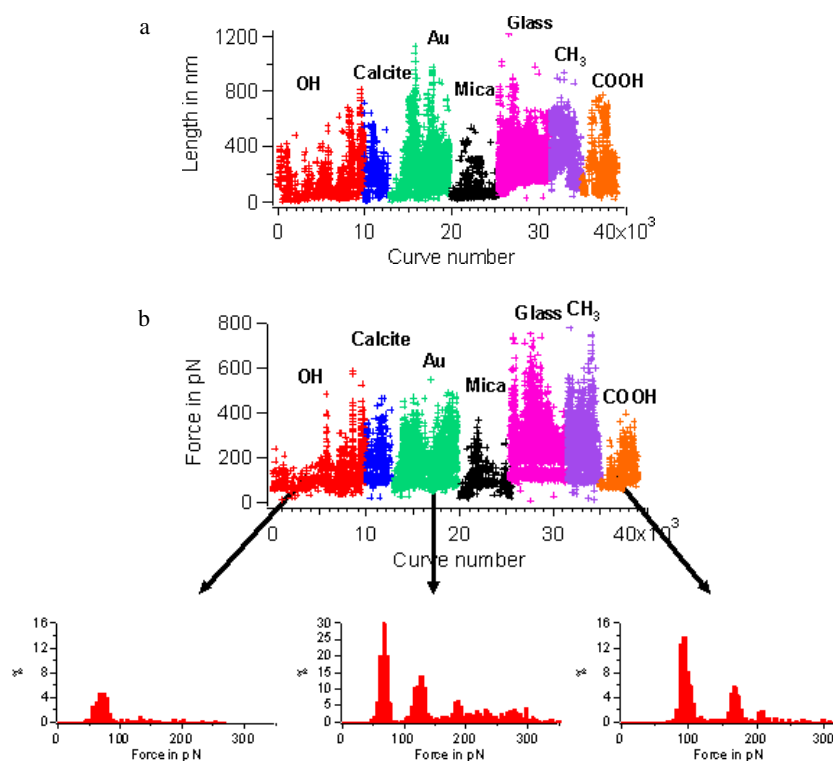


**Figure 5.** Long-term measurement with a polyacrylic acid functionalized tip on various surfaces. The measurements were done with  $\text{CaSO}_4$  in solution with concentrations varied between 0.05 and 5 mM except for the COOH and the  $\text{CH}_3$  SAM. At the highest concentration the pH was varied from 3 to 10 for every substrate—except for calcite. In most cases a set of 500 curves was recorded for each ion concentration and each pH. The dashed lines indicate when a pH variation starts and when the sample was changed. (a) The desorption lengths which are given by the lengths of the measured desorption plateaux are plotted against their curve number. During the whole measurement no systematic degradation could be observed. (b) Desorption forces corresponding to the measurements shown in figure 5(a) plotted against their curve number. Histograms for the desorption forces are extracted in the beginning, in the middle and at the end of the measurement to show the constant quality of the experimental results. In each case 500 forces spectra contribute to the desorption force histograms. The first histogram belongs to the initial measurement on the OH-SAM, the second one to the measurement on gold and the last one to the measurement on the COOH-SAM. Also for the polyacrylic acid well-defined histograms were obtained. The number of desorption events fluctuates strongly when the substrate is changed. But here also, no decreasing tendency over the course of time can be observed.

the solid substrate. Occasionally, additional peaks at higher forces appear which belong to the desorption of two or more polymer strands in parallel. As the distributions remain narrow and well defined during the whole measurement, the occurrence of significant contaminations can be excluded. As can also be seen from figure 5 the number of adsorption events remains constant during the entire experiment. Therefore one can conclude that even after 40 000 force spectra the polymers remained stably attached to the tip.

#### 4. Theoretical considerations

Several theoretical treatments exist that have been worked out to describe polyelectrolyte desorption from solid supports [23–29]. Here we present a very simplified approach that can easily be probed by force spectroscopy experiments.



The electrostatic contribution to the desorption force has been derived in the following way [21, 72]:

The electrostatic potential  $V^{\text{el}}(z)$  of the substrate in the Debye–Hückel approximation is given by:

$$\frac{eV^{\text{el}}(z)}{k_{\text{B}}T} = 4\pi l_{\text{B}}\sigma\kappa^{-1}e^{-\kappa z} \quad (1)$$

where  $k_{\text{B}}$  is the Boltzmann constant,  $T$  is the temperature,  $\sigma$  is the surface charge density of the substrate,  $\kappa^{-1}$  is the Debye screening length and  $l_{\text{B}}$  is the Bjerrum length that signifies the distance at which the electrostatic interaction of two unit charges,  $e$ , in a solvent without counter ions equals the thermal energy  $k_{\text{B}}T$ .

The force that is required to pull the polymer away from the surface over the length of one polymer segment equals the force that is needed to transport one charged segment from  $z = 0$  to  $\infty$ :

$$F_{\text{des}}^{\text{el}} = \frac{[\phi(\infty) - \phi(0)]\tau a}{a} = (4\pi l_{\text{B}}k_{\text{B}}T)\sigma\kappa^{-1}\tau \quad (2)$$

where  $\tau$  signifies the line charge density of the polyelectrolytes and  $a$  means the monomer length.

Also non-electrostatic contributions are involved in the adsorption process. As a first approximation these non-electrostatic contributions can be modelled in a constant additive term to obtain the following expression for the desorption force:

$$F_{\text{des}} = F_0 + (4\pi l_{\text{B}}k_{\text{B}}T)\sigma\kappa^{-1}\tau. \quad (3)$$

As can be seen from equation (3) the desorption force depends linearly on the Debye screening length if electrostatic interactions are involved in the desorption process. The linear dependence can easily be probed *in situ* by varying the salt concentration in solution. Thus this approach can be utilized to discriminate between Coulombic and non-Coulombic interactions.

## 5. Coulombic contributions

The linear dependency on the Debye screening length was first validated by desorption measurements with positively charged polyelectrolytes, e.g. polyvinylamine on different negatively charged surfaces including calcite and mica [20–22]. With the negatively charged polyacrylic acid for the first time repulsive electrostatic interactions were probed as well as attractive interactions [22].

Two examples that prove electrostatic interactions for polyacrylic acid are shown in figure 6. Figure 6(a) shows a graph that corresponds to measurements that were performed with a varied NaCl concentration at pH 6 on silicon functionalized with quaternary amines which therefore carried a permanent positive charge. The mean desorption forces for one single polyacrylic chain was determined by analysing the first peak in the histogram of the desorption forces found for a certain NaCl concentration. These desorption forces were then plotted against their Debye screening length. The desorption force was found to linearly increase with the Debye screening length, indicating an attractive force that is increasingly screened when the NaCl concentration is increased. Figure 6(b) shows the results for the slightly negatively charged calcite. In this case the desorption force decreases linearly with the Debye screening length, which indicates a repulsive interaction between the polyacrylic acid strands and the calcite surface. These results show how electrostatic interaction can be identified by analysing the relationship between the mean desorption force and the Debye screening length. Further information can be extracted, e.g. the surface charge density of the investigated surface can be

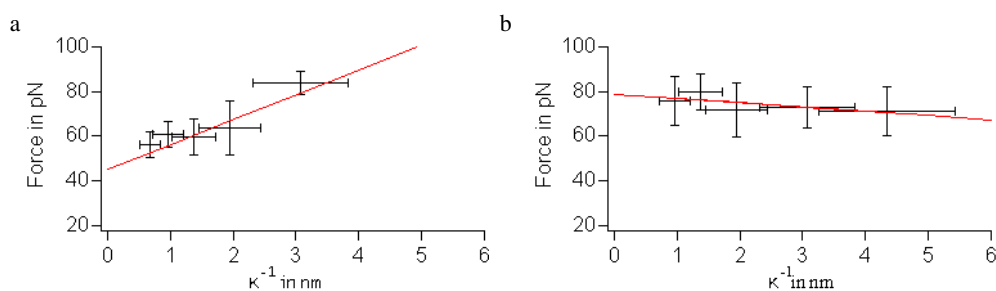


**Figure 6.** Monitoring of electrostatic interactions between polyacrylic acid and two surfaces carrying surface charge of different signs. (a) Measurements on aminofunctionalized silicon, that is positively charged, with NaCl in solution. The mean desorption force depends linearly on the Debye screening length. The straight line is rising which indicates an attractive interaction because the desorption force decreases when the salt concentration is increasing. (b) Measurements on calcite, that represents a slightly negatively charged surface, with NaCl in solution. The mean desorption force depends linearly on the Debye screening length adjusted by the NaCl concentration in the solution. The falling straight line indicates a repulsive interaction: the desorption force is increasing with increasing salt concentration.

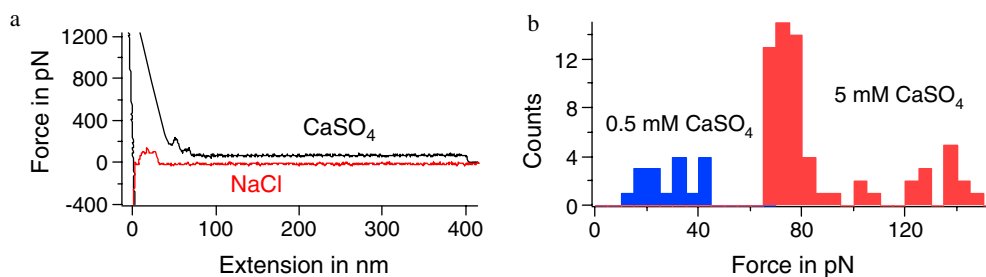


**Figure 7.** Desorption measurements with polyacrylic acid on mica. (a) Force-extension curves for 100 mM NaCl (black) and 0.5 mM CaSO<sub>4</sub> (grey). Even at high concentrations of NaCl it is not possible to observe the desorption of single polyacrylic acid chains whereas even at small concentrations of CaSO<sub>4</sub> desorption plateaux can be observed. (b) Desorption force histograms for different concentrations of CaSO<sub>4</sub>. The desorption force as well as the number of desorption events strongly increases when the CaSO<sub>4</sub> concentration is raised from 0.5 to 5 mM.

determined if the line charge density of the polyelectrolyte is known, or, if the same surface is probed with different weak polyelectrolytes, their degree of dissociation can be compared which is in general an unknown size for polyelectrolytes facing a charged surface.

If the same desorption experiment is carried out with mica [22], which represents a stronger negatively charged surface than calcite, no adhesion of the negatively charged polyacrylic acid was observed with NaCl in solution. Only under strong screening conditions ( $c_{\text{NaCl}} = 100 \text{ mM}$ ) are short range attractions between the polyacrylic acid coated AFM-tip and the mica surface observed, but no long desorption plateaux that would represent the desorption of a single polyacrylic chain were found. This fact is due to the stronger electrostatic repulsion that could not be screened by the salt in solution. If the measurements were done with CaSO<sub>4</sub> in solution, even small salt-concentrations ( $\sim 0.5 \text{ mM}$ ) could enable the adsorption of polyacrylic acid chains on the mica surface. The desorption force was found to be increasing when the CaSO<sub>4</sub> concentration was increased. The results for mica are summarized in figure 7. Their interpretation still requires further investigation but they corresponds well to the known effect of induced polyanion binding by multivalent cations.

## 6. Non-Coulombic contributions

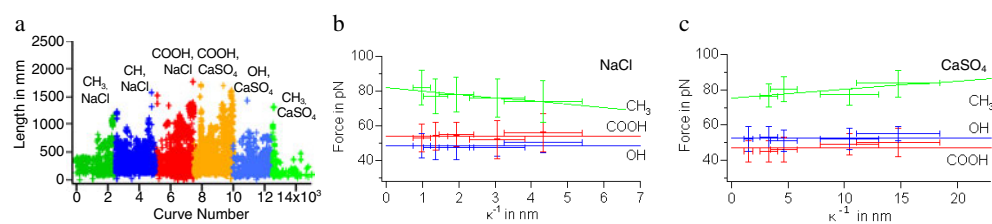
While Coulombic contributions can easily be identified and characterized by the investigation of the relationship between the mean desorption force and the Debye screening length that is determined by the salt concentration in solution, the investigation of the constant term in equation (3) is much more difficult. This is due to the fact that the non-Coulombic off-set  $F_0$  in general consists of different contributions, e.g. van der Waals interactions, coordinative bonds or hydrogen bonds, that are hard to separate from each other. Nevertheless some of them can be identified by the analysis of differences in the adsorption characteristics induced by certain environmental changes. One example of such a systematic investigations are desorption measurements of polyacrylic acid on self-assembled monolayers (SAMs) [73]. The SAMs consisted of  $\text{CH}_3$ -terminated, OH-terminated and COOH-terminated alkylchains that represent a hydrophobic, a polar and an acidic surface<sup>1</sup>, respectively<sup>2</sup>. The measurements were carried out with the same AFM-tip, so that the results can be directly compared, with various salt-concentrations of NaCl and  $\text{CaSO}_4$  in solution at pH 6. In order to come to a conclusive result many different facts have to be taken into consideration as will be shown in the following.

Figure 8 gives an overview of the sequence and the main results of such an experiment performed with the same set of molecules: in figure 8(a) the lengths of all desorption plateaux found during the whole measurement were determined as described in section two and plotted against their curve number. First the ion concentration of NaCl was varied for  $\text{CH}_3$ -SAM (curve number 0–2500), then the same was done for OH-(curve number 2500–5000) and COOH-SAM (curve number 5000–7500). Then the SAMs were probed in the reverse order with varied concentrations of  $\text{CaSO}_4$  in solution (COOH-SAM: curve number 7500–10000, OH-SAM: curve number 10000–12500,  $\text{CH}_3$ -SAM: curve number 12500–15000). As can be seen in the figure, for both ions only short plateaux were found on the  $\text{CH}_3$ -SAM, longer ones on the OH-SAM and the longest ones on the COOH-SAM. The mean desorption forces found for the three different SAM-substrates were extracted from the histograms by a Gaussian fit of the first peak. In figures 8(b) and (c) they are plotted against their Debye screening length. A linear dependency of the desorption force on the salt concentration was only found in the case  $\text{CH}_3$ -SAM, as can be seen in figures 8(b) and (c): the desorption force was found to be increasing with the Debye screening length for NaCl and decreasing for  $\text{CaSO}_4$ . The first case corresponds to a repulsive electrostatic contribution which indicates a negative surface charge of the  $\text{CH}_3$ -SAM. This is well in agreement with measurements performed by Schweiss *et al* who determined the surface potential of a  $\text{CH}_3$ -terminated SAM to be  $\sim -70$  mV by  $\zeta$ -potential measurements [74]. The negative potential is attributed to adsorbed hydroxide ions at the SAM-surface. The results for  $\text{CaSO}_4$  in solution indicate an attractive electrostatic interaction. This could be mediated by Ca ions bound to the carboxylgroups of the polyacrylic acid. For the OH- and the COOH-SAM no significant dependence on the Debye screening length was found<sup>3</sup>. This means that the adsorption is dominated by non-Coulombic interactions for these surfaces. The desorption forces for the COOH- and the OH-SAM lie in the same range for both ions ( $\sim 50$  pN), whereas for both ions the desorption force is significantly

<sup>1</sup> There are several values for the  $pK_a$  of the COOH-terminated SAM in the literature ranging from 5 to 11 and therefore it is rather unclear if the carboxyl-groups are deprotonated or not. Further investigations of our SAM-samples revealed  $pK_a$  values ranging from 8 to 10. Therefore the extent of deprotonated groups is expected to be rather low.

<sup>2</sup> Details of the SAM-preparation are given in [73].

<sup>3</sup> For all three SAM samples the electrostatic contribution that could be identified was much weaker than expected. One possible explanation for this could be the fact that the same samples provide an interface with a low dielectric constant so that the carboxylgroups of the polyacrylic acid molecules become protonated due to repulsive image charge interactions. This feature will be discussed in more detail in a separate publication.



**Figure 8.** Overview of all desorption lengths and desorption forces for single polyacrylic acid molecules measured on the three different thiol SAM-samples. In figure 4(a) the lengths of all plateaux found in the whole measurement are plotted against their curve number. In figures 4(b) and (c) all desorption forces found for different concentrations of NaCl and CaSO<sub>4</sub> are depicted against the Debye screening length. The straight lines signify the linear smoothing functions. (a) Desorption lengths for the whole data set. The first three blocks represent the measurements with varied NaCl concentrations on the three different SAMs, the last three blocks represent the measurements with varied CaSO<sub>4</sub> concentrations. For NaCl as well as for CaSO<sub>4</sub> the shortest plateaux were found for the CH<sub>3</sub>-SAM. For the OH-SAM in both cases longer plateaux also appear, while the longest desorption plateaux for both ions were found for the COOH-SAM. (b) Measurements with NaCl in solution. The non-Coulombic contribution to the desorption force for the OH-SAM (48 pN) is the lowest. The non-Coulombic contribution for the COOH-SAM is slightly higher (54 pN) while the one for the CH<sub>3</sub>-SAM is remarkably higher (77 pN). In the case of the CH<sub>3</sub>-SAM a repulsive electrostatic interaction can be identified. (c) Measurements with CaSO<sub>4</sub> in solution. The non-Coulombic contribution to the desorption force for the OH-SAM is slightly increased (53 pN) compared to the one with NaCl in solution and is slightly higher than the non-Coulombic contribution measured on the COOH-SAM (47 pN) that is decreased compared to the one measured with NaCl in solution. The non-Coulombic contribution for the CH<sub>3</sub>-SAM is nearly unchanged (79 pN) and is again remarkably higher than the one measured for the other SAMs. In the case of the CH<sub>3</sub>-SAM an attractive electrostatic interaction can be identified. The desorption force on the other SAMs is salt-independent.

higher on the CH<sub>3</sub>-SAM (~80 pN). Additional facts can be extracted by having a closer look at the desorption force histograms: three of them, representative for the measurements on the CH<sub>3</sub>-, the OH- and the COOH-SAM are shown in figure 9. For the CH<sub>3</sub>-SAM only one peak appears to correspond to the desorption of a single polyelectrolyte chain of the SAM-surface, whereas for the OH-SAM a second peak, and for the COOH-SAM at least a third peak, can be identified, which represent the desorption of two and three polyelectrolyte strands in parallel, respectively. The number of desorption events found in a set of 500 force-extension curves was rather small for the CH<sub>3</sub>-SAM (~30%), larger for the OH-SAM (~100%) and largest for the COOH-SAM (~200%). This holds for the total number of desorption events as well as for single and multiple peaks in the force histograms, as can be seen from figure 9.

The assumption that the water close to the OH- and the COOH-SAM is assumed to be a better solvent for the polyacrylic acid than it is at the CH<sub>3</sub>-SAM interface was found to be consistent with all the experimental findings listed above. If the quality of the solvent is poor at the SAM-water interface the probability that the polyelectrolyte traverses the interface to adsorb on the SAM is lowered. This could explain why fewer desorption events were observed for the CH<sub>3</sub>-SAM. In addition, the fact is taken into consideration that it is more probable for the short polymer molecules to desorb from the SAM on the AFM-tip and cross the barrier at the SAM-water interface to adsorb onto the SAM-surface opposing the tip. The same argument accounts for the finding that no longer desorption plateaux were observed on the CH<sub>3</sub>-SAM. Once a molecule has succeeded in adsorbing onto the CH<sub>3</sub>-SAM it is nevertheless hindered by the bad solvent to desorb and traverse the SAM-water interface again. Thus high desorption forces are expected, as observed in the experiment. For the OH- and the COOH-SAM the opposite considerations can be accomplished. This scenario is summarized in figure 10.

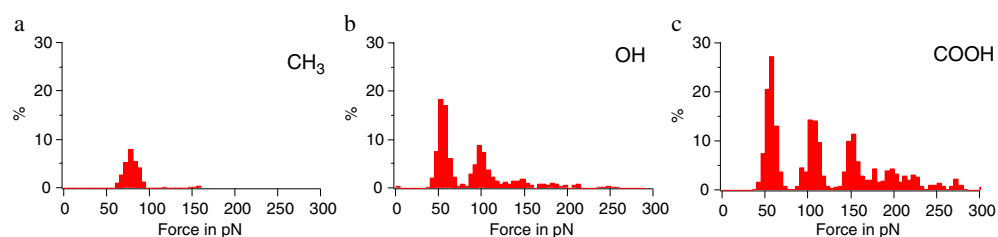


**Figure 9.** Histograms for the desorption forces of polyacrylic acid measured for the three substrates. The height of the desorption plateaux found in the force-extension curves represents the desorption force. The first peak in the histograms corresponds to the desorption of single molecules, the following peaks to the desorption of two or more molecules. All histograms represent measurements done with NaCl in solution and were determined by the analysis of a set of 500 force-extension curves that were recorded with a constant salt concentration. The histograms were normalized to the number of measured force curves, so that the height of the bars represents the portion of desorption plateaux of a particular height found in a set of 500 force curves. (a) CH<sub>3</sub>-SAM: only one peak appears that corresponds to the desorption of a single molecule. Compared to the OH- and the COOH-SAM fewer desorption plateaux were found in the data set and the distribution of the desorption forces is rather broad. (b) OH-SAM: two peaks can be clearly identified that correspond to the desorption of one and two polymer molecules, respectively. More desorption plateaux were found than in the case of the CH<sub>3</sub>-SAM and the peaks are better defined. (c) COOH-SAM: three peaks can be distinguished that correspond to the desorption of one, two and three polyacrylic acid molecules. The peaks are well defined and a large number of desorption plateaux is found in the data set.

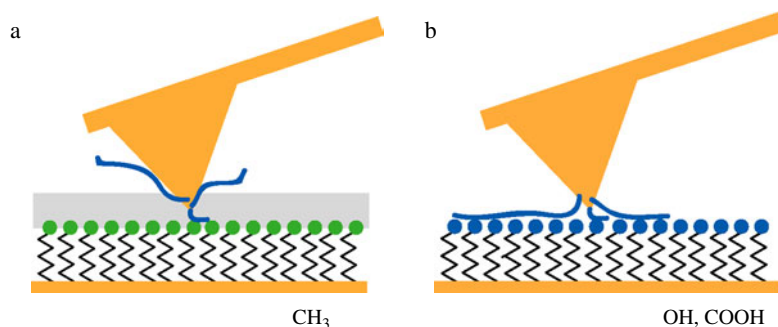


**Figure 10.** Effect of the solvent quality at the SAM-water interface. (a) Bad solvent for the polyacrylic acid: especially the longer strands do not pass the interface to adsorb on the opposing surface. If a molecule nevertheless has reached the SAM surface it is hindered by the bad solvent to traverse the interface again and desorb from the SAM-surface. (b) Good solvent at the interface: the probability that molecules pass the interface is increased. Also the longer molecules adsorb on the SAM surface. The good solvent also facilitates the way back from the SAM surface to the tip and therefore desorption is easier and occurs at lower forces.

Assuming that in a zero order approximation the surface free energy of the air water interface is comparable to that of the interface between water and the methyl endgroups of a SAM, the surface tension of a saturated PAA solution was measured relative to that of pure water. The measured value of  $30 \pm 3 \text{ mJ m}^{-2}$  was used to estimate the resulting desorption force to be  $F_{\text{des}} \approx 10 \text{ pN}$ . This corresponds very well to the experimentally determined difference between the desorption forces on the hydrophobic CH<sub>3</sub>-SAM and the hydrophilic OH- or COOH-SAMs and is also in accordance with other investigations concerning the structure of water at SAM-interfaces [75–78]. Since Coulomb and van der Waals interactions on all surfaces are expected to be comparable, this difference must be attributed to hydrophobic

effects and thus to a difference in the structure of water at the different SAM interfaces. This is one example where one contribution to the non-Coulombic interaction was determined by varying the substrate and comparison of the results. Variation of the pH, of the solvent or of the adsorbing polyelectrolyte would be alternative approaches to identifying other non-Coulombic contributions.

## 7. Concluding remarks

Single molecule force spectroscopy was successfully applied to study the desorption process of single polyelectrolyte chains from solid supports. Long-term measurements allow a precise investigation of polyelectrolyte desorption under various environmental conditions. Coulombic and non-Coulombic contributions could be separated and a variety of different interactions could be characterized that reveal valuable details about the adsorption process and reflect the characteristic properties of the investigated surface. Thus desorption experiments provide a versatile tool to probe theoretical predictions, and in addition they represent a way of utilizing single polymer molecules as suitable sensors which allow the investigation and characterization of generic surfaces.

## Acknowledgments

This work was supported by the Deutsche Forschungsgemeinschaft (DFG) through SFB 486. Helpful discussions with Roland Netz are thankfully acknowledged.

## References

- [1] Oosawa F 1971 *Polyelectrolytes* (New York: Dekker)
- [2] Dautzenberg H, Jaeger W, Kötz B P J, Seidel C and Stscherbind D 1994 *Polyelectrolytes: Formation, Characterization and Application* (Munich: Hanser Publishers)
- [3] Förster S and Schmidt M 1995 *Adv. Polym. Sci.* **120** 50
- [4] Hesselink T T 1977 *J. Colloid Interface Sci.* **60** 448
- [5] Fleer G J and Lyklema J 1974 *J. Colloid Interface Sci.* **167** 228
- [6] Matsumoto T and Adachi Y 1998 *J. Colloid Interface Sci.* **204** 328
- [7] Horn D and Roberts Linkart F (ed) 1996 *Paper Chemistry* (Glasgow: Blackie Academic & Professional)
- [8] Mann S 1988 *Nature* **332** 119
- [9] Mann S, Webb J and Williams R J P 1989 *Biom mineralization: Chemical and Biochemical Perspectives* (Weinheim: VCH)
- [10] Addadi L and Weiner S 1992 *Angew. Chem.* **104** 159
- [11] Qi L, Cölfen H and Antonietti M 2000 *Angew. Chem.* **112** 617
- [12] Wong J Y, Majewsky J, Seitz M, Park C K, Israelachvili J N and Smith G S 1999 *Biophys. J.* **77** 1445
- [13] Schmitt J, Grünwald T, Kjaer K, Pershan P, Decher G and Lösche M 1993 *Macromolecules* **26** 7058
- [14] Rädler J, Koltover I, Salditt T and Safinya C 1997 *Science* **275** 810
- [15] Hartley P G and Scales P J 1998 *Langmuir* **14** 6948
- [16] Caruso F, Furlong D N, Ariga K, Ichinose I and Kunitake T 1998 *Langmuir* **14** 4559
- [17] Clausen-Schauman H and Gaub H E 1999 *Langmuir* **15** 8246
- [18] Dahlgren M A G and Claesson P M 1993 *Prog. Colloid Polym. Sci.* **93** 206
- [19] Kamiyama Y and Israelachvili J 1992 *Macromolecules* **25** 5081
- [20] Senden T J, di Meglio J M and Auroy P 1998 *Eur. Phys. J. B* **3** 211
- [21] Hugel T, Grosholz M, Clausen-Schaumann H, Pfau A, Gaub H E and Seitz M 2001 *Macromolecules* **34** 1039
- [22] Seitz M, Friedsam C, Jöstl W, Hugel T and Gaub H E 2003 *Chem. Phys. Chem.* **4** 986
- [23] Netz R R and Orland H 1999 *Eur. Phys. J. B* **8** 81
- [24] Netz R R and Joanny J-F 1999 *Macromolecules* **32** 9013
- [25] Livadaru L, Netz R R and Kreuzer H J 2003 *Macromolecules* **36** 3732
- [26] Khokhlov A R and Khachaturian K A 1982 *Polymer* **23** 1742



- [27] Fleck C, Netz R R and von Grünberg H H 2002 *Biophys. J.* **82** 76
- [28] Netz R R 2003 *J. Phys.: Condens. Matter* **15** S239
- [29] Barrat J-L and Joanny J-F 1996 *Adv. Chem. Phys.* **94** 1
- [30] Decher G 1997 *Science* **277** 1232
- [31] Lösche M, Schmitt J, Decher G, Bouwman W G and Kjaer K 1998 *Macromolecules* **31** 8893
- [32] Caruso F, Caruso R A and Möhwald H 1998 *Science* **282** 1111
- [33] Donath E, Sukhorukov G B, Caruso F, Davis S A and Möhwald H 1998 *Angew. Chem. Int. Edn Engl.* **16** 37
- [34] Fang Y and Yang J 1997 *J. Phys. Chem. B* **101** 441
- [35] Salditt T, Koltover I, Rädler J O and Safinya C R 1997 *Phys. Rev. Lett.* **79** 2582
- [36] Maier B and Rädler J O 1999 *Phys. Rev. Lett.* **82** 1911
- [37] von Berlepsch H, Burger C and Dautzenberg H 1998 *Phys. Rev. E* **58** 7549
- [38] Anghel D G, Saito S, Baran A and Iovescu A 1998 *Langmuir* **14** 5342
- [39] Clark S L and Hammond P T 2000 *Langmuir* **16** 10206
- [40] Smith S B, Finzi L and Bustamante C 1992 *Science* **258** 1122
- [41] Ashkin A, Schütze K, Dziedzic J M, Euteneuer U and Schliwa M 1990 *Nature* **348** 346
- [42] Kishino A and Yanagida T 1988 *Nature* **334** 74
- [43] Evans E, Ritchie K and Merkel R 1995 *Biophys. J.* **68** 2580
- [44] Binnig G, Quate C F and Gerber C 1986 *Phys. Rev. Lett.* **56** 930
- [45] Rief M, Oesterhelt F, Heymann B and Gaub H E 1997 *Science* **275** 1295
- [46] Clausen-Schaumann H, Seitz M, Krautbauer R and Gaub H E 2000 *FEBS Lett.* **510** 154
- [47] Thomson N H, Fritz M, Radmacher M, Schmidt C F and Hansma P K 1996 *Biophys. J.* **70** 2421
- [48] Strunz T, Oroszlan K, Shafer R and Güntherodt H-J 1999 *Proc. Natl Acad. Sci. USA* **96** 11277
- [49] Krüger D, Fuchs H, Rousseau R, Marx D and Parrinello M 2002 *Phys. Rev. Lett.* **89** 186
- [50] Allemand J-F, Bensimon D, Jullien L, Bensimon A and Croquette V 1997 *Biophys. J.* **73** 2064
- [51] Florin E L, Moy V T and Gaub H E 1994 *Science* **264** 415
- [52] Dammer U, Hegner M, Anselmetti D, Wagner P, Dreier M, Huber W and Güntherodt H-J 1996 *Biophys. J.* **70** 2437
- [53] Dettmann W, Grandbois M, André S, Benoit M, Wehle A K, Kaltner H, Gabius H-J and Gaub H E 2000 *Arch. Biochem. Biophys.* **383** 157
- [54] Grandbois M, Beyer M, Rief M, Clausen-Schaumann H and Gaub H E 1999 *Science* **283** 1727
- [55] Merkel R, Nassoy P, Leung A, Ritchie K and Evans E 1999 *Nature* **397** 50
- [56] Evans E and Williams P 2002 *Dynamic Force Spectroscopy: I. Single Bonds* (Berlin: Springer)
- [57] Evans E and Ritchie K 1997 *Biophys. J.* **72** 1541
- [58] Grubmüller H, Heymann B and Tavan P 1996 *Science* **271** 997
- [59] Heymann B and Grubmüller H 2000 *Phys. Rev. Lett.* **84** 6126
- [60] Israilev S, Stepaniants S, Balsera M, Ono Y and Schulten K 1997 *Biophys. J.* **72** 1568
- [61] Friedsam C, Wehle A K, Kühner F and Gaub H E 2003 *J. Phys.: Condens. Matter* **15** S1709
- [62] Dettmann W, Grandbois M, André S, Benoit M, Wehle A, Kaltner H, Gabius H-J and Gaub H E 2000 *Arch. Biochem. Biophys.* **383** 157
- [63] Kacher C M, Weiss I K, Stewart R J, Schmidt C F, Hansma P K, Radmacher M and Fritz M 2000 *Eur. Biophys. J.* **28** 611
- [64] Silberzan P, Léger L, Ausserré D and Benattar J J 1991 *Langmuir* **7** 1647
- [65] Tripp C T and Hair M L 1992 *Langmuir* **8** 1120
- [66] Angst D L and Simmons G W 1991 *Langmuir* **7** 2236
- [67] Ulman A 1996 *Chem. Rev.* **96** 1533
- [68] Nuzzo R G and Allara D L 1983 *J. Am. Chem. Soc.* **105** 4481
- [69] Whitesides G M and Laibinis P E 1990 *Langmuir* **6** 87
- [70] Dubois L H and Nuzzo R G 1992 *Annu. Rev. Phys. Chem.* **43** 437
- [71] Friedsam C, Gaub H E and Seitz M 2003 *Chem. Phys. Chem.* **5** 388–93
- [72] Israelachvili J 1992 *Intermolecular and Surface Forces* (New York: Academic)
- [73] Friedsam C, Gaub H E and Seitz M 2003 *New J. Phys.* **6** 9
- [74] Schweiss R, Welzel P B, Werner C and Knoll W 2001 *Langmuir* **17** 4304
- [75] Schwendel D, Hayashi T, Dahint R, Pertsin A, Grunze M, Steitz R and Schreiber F 2003 *Langmuir* **19** 2284
- [76] Chan Y-H M, Schweiss R, Werner C and Grunze M 2003 *Langmuir* **19** 7380
- [77] Herrwerth S, Eck W, Reinhardt S and Grunze M 2003 *J. Am. Chem. Soc.* **125** 9359
- [78] Mamatkulov S I, Khabibullaev P K and Netz R R 2003 at press